# Design Guidelines for Processing Bi-Material Components via Powder-Injection Molding

John L. Johnson, Lye King Tan, Pavan Suri, and Randall M. German

*Powder injection molding can be used to fabricate bi-material components that provide unique functionality such as a combination of toughness and wear resistance. Successful processing of these components requires minimization of internal stresses during sintering. In this article, the stresses generated during co-sintering of concentric rings are analyzed, compared to the materials' strengths, and correlated with defects. The results provide guidelines for determining the compatibility of various materials and the effect of component geometry.*

## INTRODUCTION

Net shaping significantly reduces the cost of realizing complex engineering designs, and a variety of manufacturing routes have emerged that eliminate machining and increase savings. One newer high-productivity, high-performance net-shaping method geared to complex shapes is powder-injection molding (PIM), which relies on plastic forming equipment to shape powder. A lubricating polymer phase is added for molding and then is extracted by heat prior to sinter densification of the powder. Today, most sintered products match the density and properties attained from casting or machining. As long as the mold is oversized, the final product meets specifications without machining.

Effectively, PIM provides the geometric shape attributes associated with plastic injection molding and the performance attributes associated with full-density powder metallurgy and ceramic sintering. Already, PIM has secured impressive gains in the production of components for computer disk drives, cellular telephones, dental orthodontics, surgical tools, investment casting cores, military and sporting firearms, wrist watches, and a broad array of automotive and industrial applications. The technology has excelled in the mass production of complicated shapes from materials that are difficult to cast or machine.

To date, PIM applications have been restricted to monolithic materials such as low-alloy steels, stainless steels, alumina or silica, tungsten alloys, titanium, cemented carbides, or controlled expansion alloys such as Kovar or Invar. After fabrication, the PIM product is usually combined with another component to form an assembly. Since sintering is performed at temperatures where diffusion bonding is possible, a goal in PIM has been to form green assemblies (by joining prior to sintering) and use the sintering step for diffusion bonding.

In further PIM evolution, the green assembly is performed directly in molding using a technology known as bi-material PIM.[1–3] If two feedstocks of differing materials can be designed to co-sinter, then two-color plastic molding technology can be employed to form the assembly in the molding step. The intent is to generate bi-material net-shape structures with properties tailored to a wide range of applications, in such combinations as:

- Magnetic and non-magnetic
- Magnetic response and corrosion resistance
- Controlled porosity and high thermal conductivity
- High inertial weight and high strength

**Table I. Equations**

$$\sigma_{r,max} = \frac{E\delta}{2c}\frac{c^2 - a^2}{b^2 - a^2}\left(1 - \frac{b^2}{c^2}\right) \quad (1)$$

$$\sigma_i = \sigma_y(T)\cdot\frac{N_c \cdot V_s}{k\pi}\cdot\left(\frac{X}{D}\right)^2 \quad (2)$$

$$\sigma_{h,outer,max} = \frac{E\delta}{2c}\frac{c^2 - a^2}{b^2 - a^2}\left(1 + \frac{b^2}{c^2}\right) \quad (3)$$

$$\sigma_{h,inner,max} = \frac{E\delta}{c}\frac{b^2 - a^2}{b^2 - a^2} \quad (4)$$

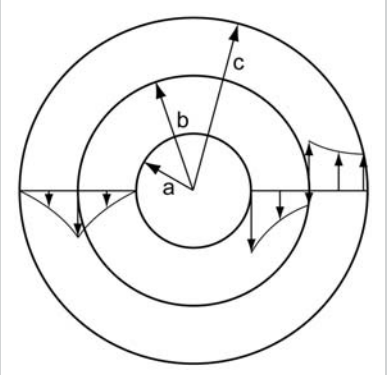


Figure 1. The radial stresses (shown on the left) and hoop stresses (shown on the right) induced in concentric ring components during processing in which the outer ring shrinks more than the inner ring.

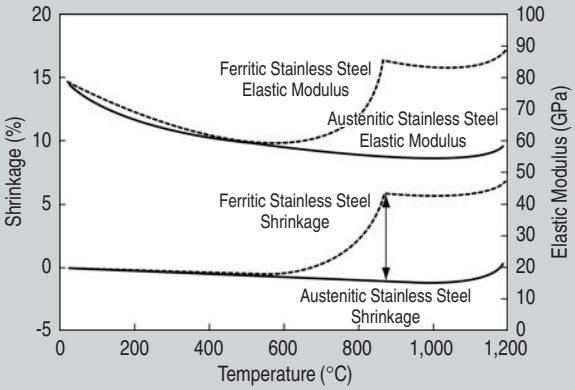


Figure 2. The temperature dependence of the elastic modulus and shrinkage for ferritic and austenitic stainless steel.

Figure 3. The interfacial separation (indicated by arrow) between an outer austenitic stainless steel ring and an inner ferritic stainless steel ring, which were two-color injection molded, debound, and vacuum sintered.

- High thermal conductivity and low thermal expansion coefficient
- Wear resistance and high toughness
- High thermal conductivity and good glass-to-metal sealing
- High elastic modulus and high damping capacity
- Magnetic response and electrical resistance

Molding two-material components with two-color molding machines commonly used in the plastics industry is relatively straightforward. An insert is injected from one material. Then, the mold is rotated and a second material is injected around the first, producing a bi-material component. The polymer is then extracted from the component using conventional solvent and thermal debinding processes. Most process difficulties are found to occur during sintering due to the large dimensional changes that take place.

The processing of bi-material components requires careful control of the sintering shrinkage of the two materials to ensure densification and bonding while avoiding differential stresses that might induce cracking or distortion. The analysis of the types of defects resulting from different combinations of materials provides guidelines for designing future components. To isolate the effects of interfacial stress on defect formation, a concentric ring geometry was selected for co-sintering trials. This geometry enables relatively easy calculation of the elastic stresses that are induced during processing and highlights typical defects such as interfacial separation and cracking. Shrinkage mismatches result in both radial stresses, which are the highest at the interface and lead to interfacial separation, as well as hoop stresses, which lead to radial cracking. These stresses are schematically illustrated in Figure 1 for the case in which the shrinkage of the outer ring is greater than the shrinkage of the inner ring. This article analyzes these stresses, compares them to the intrinsic strengths of the component materials, and demonstrates that bi-material components can be successfully processed when the induced stresses do not exceed the intrinsic strengths of the two materials.

## INTERFACIAL SEPARATION

Interfacial separation is probably the most serious defect since it indicates a lack of metallurgical compatibility between the two materials. Failure of the interface occurs when the radial stresses due to differential shrinkage exceed the interfacial strength. Differential shrinkage must be considered throughout the sintering cycle, not just at the end. In

Figure 4. Despite the lack of a gap between the alumina and austenitic stainless-steel regions of this component, which was two-color injection molded, debound, and vacuum sintered, bonding between the two regions was poor.

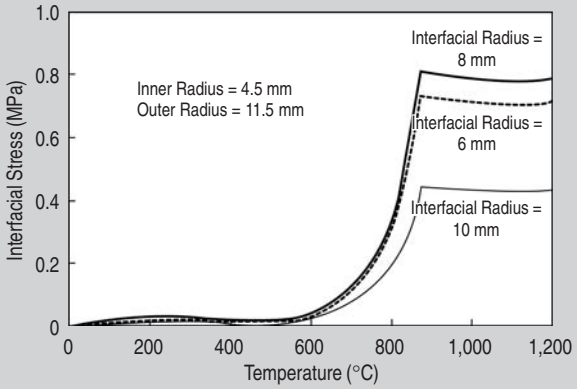


Figure 5. The effect of ring dimensions on the interfacial stress as a function of temperature.

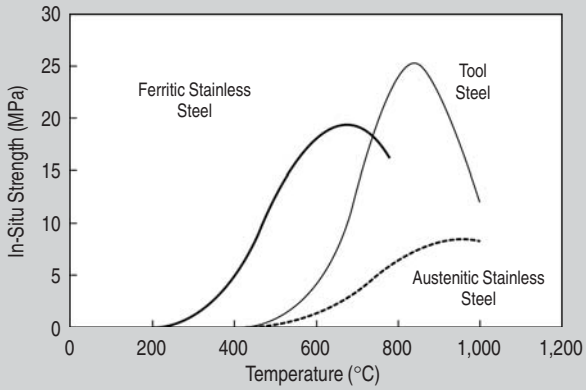


Figure 6. The evolution of the in-situ strength of three types of steel with temperature. The strength of the compacts increases with an increase in temperature due to neck growth. With a further increase in temperature, thermal softening dominates, reducing the in-situ strength of the material.

cases where bonding between the two materials is poor, the interfacial strength can be very low. Since poor bonding will result in cracking before significant plastic deformation can occur, the assumption of elastic stress is reasonable. For the concentric ring geometry, the highest radial stress occurs at the interface and is given by Equation 1[4] where a, b, and c are defined in Figure 1 and both the elastic modulus E and the mismatch strain d due to differential shrinkage are temperature-dependent terms (equations are shown in Table I). If the outer ring shrinks more than the inner ring, the mismatch strain is positive, resulting in a negative (compressive) stress. Thus, interfacial separation is only expected when the inner ring has the greater shrinkage. Examples of the temperature dependence of the elastic modulus and differential shrinkage are shown in Figure 2 for a ferritic and an austenitic stainless steel. The more open body-centered cubic structure of the ferritic stainless steel enhances densification early in the heating cycle relative to the austenitic stainless steel. As it passes through the $\alpha - \gamma$ phase transformation at 875°C, densification of the ferritic stainless steel slows to the rate of the austenitic stainless steel. The elastic modulus initially decreases with temperature due to thermal softening, but it is also porosity dependent and thus depends on the shrinkage of the material as well. As shrinkage occurs, the reduction in porosity more than compensates for thermal softening, and the elastic modulus of the material increases.

A bi-material component produced from these stainless steels results in interfacial separation (Figure 3). The greater shrinkage of the inner ring results in an interfacial stress before significant sinter bonds can form between the particles at the interface. Without these bonds, the interfacial strength is low and is exceeded by the mismatch stress, resulting in separation of the two materials during sintering.

Even if the nominal mismatch stress is practically zero, failure can still occur if the interfacial strength is very low. For example, a bi-material component can be produced from austenitic stainless steel and alumina powder as shown in Figure 4, but it displays poor bonding. Good bonding requires some chemical compatibility for interdiffusion. Materials, such as similar grades of stainless steel, that have sufficiently similar compositions to alloy together, can produce strong interfacial bonds.

Equations to describe the interfacial strength are lacking. In fact, interfacial strength is often determined by calculating the nominal mismatch stress and recognizing that the interfacial strength must be higher to produce well-bonded components.[5] The green dimensions of the component in Figures 3 and 4 are a = 4.5 mm, b = 11.5 mm, and c = 8.5 mm. The maximum radial stress calculated from Equation 1 is 0.8 MPa at 875°C. Thus, stresses of only a few MPa are sufficient to cause failure reflecting the low interfacial strength.

The geometry of the component has a significant effect on the interfacial

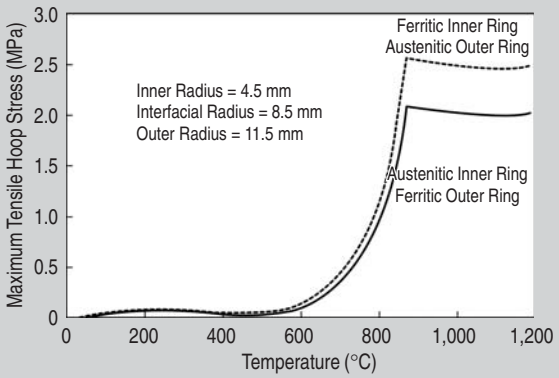


Figure 7. The effect of the relative shrinkage of the ring materials on the maximum tensile hoop stress as a function of temperature. The ferritic stainless steel has the higher shrinkage.

Figure 8. The radial cracking of stainless-steel components consisting of ring materials with different relative shrinkages. The shrinkage of the outer ring of the left component was too low, while the shrinkage of the outer ring of the right component was too high.

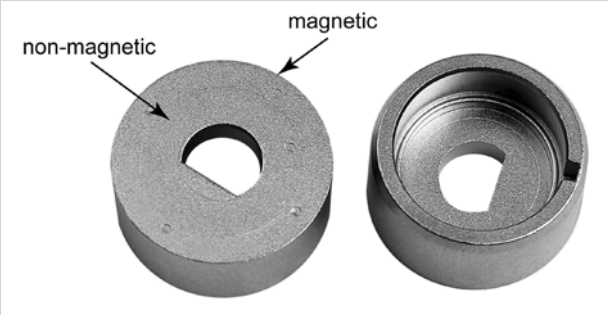


Figure 9. A production bi-material component consisting of magnetic and non-magnetic alloys is used as a holder for an angle-of-rotation sensor.

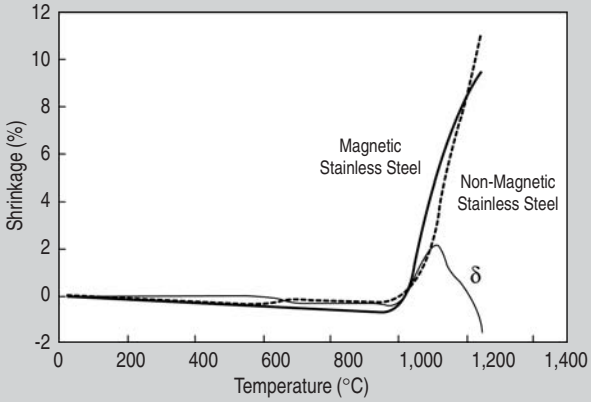


Figure 10. The temperature dependence of the shrinkage for a magnetic and non-magnetic stainless steel.

stress. The highest stresses are seen when the rings have similar thicknesses. If the outer ring is significantly thinner than the inner ring, the interfacial stress drops. This is shown in Figure 5 as a function of temperature for several geometries (ring thicknesses). Cracking can be reduced by adjusting the interfacial radius, even if the inner and outer dimensions are fixed by functional requirements of the design.

## RADIAL CRACKING

Radial cracking of one or both of the rings can occur despite metallurgical compatibility if the hoop stresses arising from shrinkage mismatch exceed the tensile strength of the material. Again, mismatch stresses and material strengths vary throughout the sintering cycle. Powder-injection molded components lose strength as the binder is removed. They reach a minimum strength once the binder is gone and before sintering begins. Fortunately, when the strength of the component is the lowest, the mismatch stress is often low due to limited dimensional change. As necks develop between particles, their strength increases, reaches a maximum, and then decreases as the material thermally softens. During sintering, the in-situ strength after binder removal is given by Equation 2[6] where $\sigma_y(T)$ is the temperature-dependent yield stress of the bulk material, $N_c$ is the coordination number, $V_s$ is the fractional density, k is a stress-concentration factor, X is the neck size, and D is the particle diameter. The coordination number depends on the density, while the stress-concentration factor is a function of the X/D ratio, which can be calculated from sintering simulations.[6] A plot of the predicted in-situ strength of several materials during heating is given in Figure 6. The in-situ strength is primarily governed by the increase in the X/D ratio relative to the decrease in the inherent strength of the material.

The in-situ strength can be compared to the mismatch stress. As shown in Figure 1, the maximum tensile hoop stress is at the interface if the shrinkage of the outer ring is greater than the shrinkage of the inner ring. Assuming limited plasticity of the material again, the hoop stress in the outer ring at the interface is given by Equation 3.[4]

If the shrinkage of the inner ring is greater than the shrinkage of the outer ring, the stress states are reversed and the maximum tensile hoop stress occurs at the inner diameter of the inner ring. This stress is given by Equation 4.[4]

Figure 7 plots hoop stresses as functions of temperature using shrinkage and elastic modulus data from Figure 2. For the case in which the outer ring has the higher shrinkage, the maximum tensile hoop stress is at the interface. This stress is lower in magnitude than if the inner ring has the higher shrinkage, which places the maximum tensile stress at the inner diameter. In both cases the hoop stresses are lower than the in-situ strengths plotted in Figure 6 and no radial cracking is predicted. However, the poor metallurgical compatibility leads to interfacial separation as previously discussed.

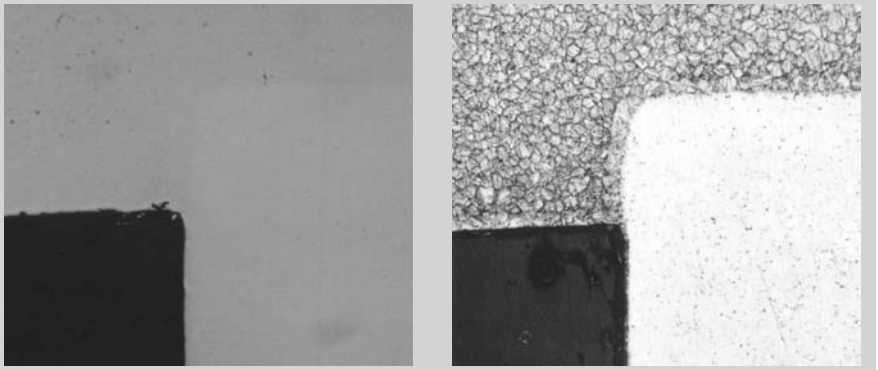

a b

Figure 11. The microstructures (a) before and (b) after etching of magnetic–non-magnetic areas in a bimetallic component.

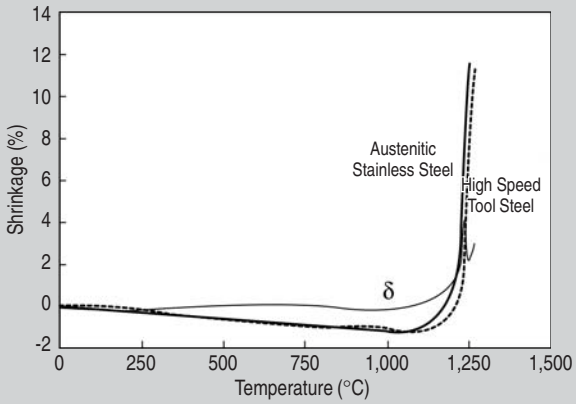


Figure 12. The temperature dependence of the shrinkage for a high-speed tool steel and an austenitic stainless steel containing 0.5 wt.% boron.

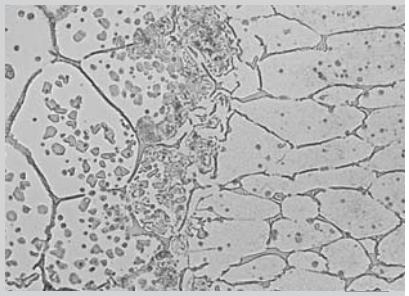


Figure 13. The microstructure of the interface between a co-sintered tool steel and an austenitic stainless steel containing 0.5 wt.% boron.

Examples of radial cracks caused by the hoop stresses are shown in Figure 8. As predicted, for the sample in which the inner ring has higher shrinkage, the crack originates from the inner diameter. For the sample in which the outer ring has higher shrinkage, the crack propagates through the ring, but likely originated at the interface. When the shrinkages of the two rings are nearly identical, a crack-free specimen can be produced.

## SUCCESSFUL DEMONSTRATIONS

By understanding the stresses involved in sintering bi-materials and how the strengths of their component materials vary during sintering, it is possible to engineer components with unique combinations of properties.

### Magnetic/Non-Magnetic

An example bi-material component consisting of magnetic and non-magnetic alloys is shown in Figure 9. Such components have applications as holders for angle-of-rotation sensors. In this case, the magnetic alloy is 17-4 PH stainless steel and the non-magnetic alloy is a modified 17-4 PH composition that contains nickel additions to stabilize the non-magnetic austenite phase. Shrinkage as a function of temperature, plotted in Figure 10, shows a good match between the two materials. Because of the similarities in the chemistry, a good metallurgical bond results between the austenitic and ferritic microstructures as shown in Figure 11.

### Tough/Wear-Resistant

Tough/wear-resistant components can be produced by co-sintering a tool steel with a stainless steel. However, chemistry modifications are needed to balance the shrinkage of these two dissimilar materials. One approach is to add boron to the stainless steel to enhance its sintering at lower temperatures. The shrinkage curve of a stainless steel containing 0.5 wt.% boron matches well with that of a tool steel, as shown in Figure 12. A good metallurgical bond forms at the interface, as shown in Figure 13.

## CONCLUSIONS

Successful processing of bi-material components requires that the interfacial strength exceed the maximum radial stress and that the in-situ material strength exceed the maximum tensile hoop stress. These requirements can be met under certain conditions. First, materials with similar compositions and powder characteristics bond well. Small modifications (less than 25%) to the powder can be used to tailor properties. This ease of modifying compositions is one of the main advantages of using PIM technology in producing metallic parts. Next, materials must have similar densification behavior for co-sintering. Minor chemistry changes can significantly alter a material's shrinkage behavior, making it more compatible for co-sintering. Shrinkage can also be adjusted by modifying the solids loading of the feedstock. Finally, component geometry can minimize internal stresses and performing stress calculations on a component can identify potential design changes to reduce the likelihood of cracking. Some design changes may not affect the external dimensions of the part, making them relatively easy to implement.

## References

1. L.K. Tan, R. Baumgartner, and R.M. German, "Powder Injection Molding of Bi-Metal Components," *Advances in Powder Metallurgy and Particulate Materials*, vol. 4, ed. W.B. Eisen and S. Kassam (Princeton, NJ: Metal Powder Industries Federation, 2001), pp. 191–198.
2. K.L. Lim et al., "Method to Form Multi-Material Components," U.S. patent 6,461,563 (8 October 2002).
3. D.F. Heaney, P. Suri, and R.M. German, "Two-Color Injection Molding of Hard and Soft Metal Alloys," *Proceedings of the 2002 International Conference on Functionally Graded Materials: Technology Leveraged Applications*, ed. R.G. Ford and R.H. Hershberger (Princeton, NJ: Metal Powder Industries Federation, 2002), pp. 105–115.
4. W.B. Bickford, *Advanced Mechanics of Materials* (Menlo Park, CA: Addison-Wesley, 1998).
5. N.E. Dowling, *Mechanical Behavior of Materials: Engineering Methods for Deformation, Fracture, and Fatigue* (Upper Saddle River, NJ: Prentice Hall, 1999).
6. X. Xu, P. Lu, and R.M. German, "Densification and Strength Evolution in Solid-State Sintering Part II," *J. of Mater. Sci.*, 37 (2002), pp. 117–126.

*John L. Johnson is R&D Manager with AMTellect in State College, Pennsylvania; Lye King Tan is senior manager, technology at Advanced Materials Technologies Pte. Ltd. in Singapore; and Pavan Suri is product development engineer and Randall M. German is director and Brush Chair Professor with the Center for Innovative Sintered Products at Pennsylvania State University.*

**For more information, contact John L. Johnson, AMTellect, 302 South Burrowes Street, State College, PA 16801; (814) 861-8090; fax (814) 861-8003; e-mail john@amtellect.com.**